

Discontinuous Transition of a Multistage Independent Cascade Model on Networks

Takehisa Hasegawa¹ and Koji Nemoto²

¹ Department of Mathematical Informatics, Graduate School of Information Science, Tohoku University, 6-3-09, Aramaki-Aza-Aoba, Sendai, Miyagi, 980-8579, JAPAN.

² Department of Physics, Hokkaido University, Kita 10 Nishi 8, Kita-ku, Sapporo, Hokkaido, 060-0810, JAPAN

E-mail: hasegawa@m.tohoku.ac.jp

E-mail: nemoto@statphys.sci.hokudai.ac.jp

Abstract. We propose a multistage version of the independent cascade model, which we call a multistage independent cascade (MIC) model, on networks. This model is parameterized by two probabilities: the probability T_1 that a node adopting a fad increases the awareness of a neighboring susceptible node, and the probability T_2 that an adopter directly causes a susceptible node to adopt the fad. We formulate a tree approximation for the MIC model on an uncorrelated network with an arbitrary degree distribution p_k . Applied on a random regular network with degree $k = 6$, this model exhibits a rich phase diagram, including continuous and discontinuous transition lines for fad percolation, and a continuous transition line for the percolation of susceptible nodes. In particular, the percolation transition of fads is discontinuous (continuous) when T_1 is larger (smaller) than a certain value. A similar discontinuous transition is also observed in random graphs and scale-free networks. Furthermore, assigning a finite fraction of initial adopters dramatically changes the phase boundaries.

1. Introduction

Word-of-mouth phenomena often catapult books, movies, and music out of obscurity and into popularity. Similar propagative effects are observed in voting behavior, the spread of rumors, and diffusion of innovations. Several models for describing such information cascades have been proposed in social science [1, 2, 3, 4, 5]. In the context of network science, Watts proposed a network model (the linear threshold model [1] on a network), in which the decision made by each node (person) to adopt an innovation is determined by the relative number of its adjacent nodes (friends) who have already adopted it [6, 7]. As the decision threshold is lowered, the model transits from the local cascade phase, where cascades are constrained, to the global cascade phase, where some small initial shocks are propagated through the whole system. This transition is discontinuous; the final fraction of adopters rises discontinuously, and its distribution over many trials is bimodal even at the transition threshold ‡. Following the seminal paper by Watts, several authors have investigated the effects of network topology on the transition threshold [8, 9, 10, 11, 12, 13].

The linear threshold model assumes *permanently active* nodes; that is, a node that has adopted an innovation will retain that innovation. On the other hand, the susceptible-infected-removed (SIR) model [14] and the independent cascade (IC) model [15, 16] (including the SIR model with transmissibility [17]) have been investigated as models of *transient fads*. In the IC model, a fad adopter abandons the fad after a single attempt, with a certain probability, to transmit the fad to each susceptible neighbor. The SIR and IC models on complex networks have been extensively studied both analytically and numerically [18, 19, 17]. On networks, the transition of these models is not discontinuous but continuous §.

Several complex contagion models have been recently reported [24, 25, 26, 27, 28, 29]. Even transient fads may undergo discontinuous transition if more than one state is available to each node before adoption. Incorporating *social reinforcement* into the SIR model, Krapivsky et al. developed an agent-based model of transient fads, which we call the fad model [28]. Here, social reinforcement means that each node adopts a fad only after multiple prompts from adjacent adopters. In this model, a node takes one of the $M + 1$ awareness levels $(0, 1, \dots, M)$: Nodes with the awareness level less than M remain susceptible, and nodes with the highest awareness level M adopt the fad. Each adopter increases the awareness level of its adjacent neighbors by one at a unit rate. Adopters also abandon the fad at a certain rate. In the absence of reinforcement ($M = 1$), the model reduces to an ordinary SIR model. Krapivsky et al. studied this

‡ Watts claimed that the linear threshold model on networks show both continuous (in a low connectivity region) and discontinuous (in a high connectivity region) transitions [6]. The continuous transition is essentially due to the percolation of underlying network, and the model is expected to show only discontinuous transition if the network has sufficient connectivity.

§ The SIR model is mapped onto the IC model with a transmission probability (the SIR model with transmissibility). Although these two behave differently from each other on local scales, there is a correspondence between these two for critical points and critical exponents [20, 21, 22, 23].

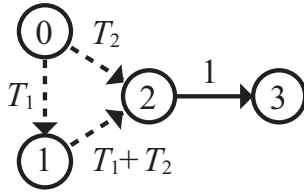


Figure 1. Transition rules of the present MIC model. The values on the lines indicate the transmission probability. The events indicated by the dashed lines ($0 \rightarrow 1$, $0 \rightarrow 2$, and $1 \rightarrow 2$) occur at nodes adjacent to an adopter. The event indicated by the solid line ($2 \rightarrow 3$) occurs irrespective of the neighbor's state.

model without a spatial structure by the macroscopic rate equations [28]. They showed that the transition is continuous for $M = 1$ and discontinuous for $M \geq 2$. However, the behavior of this agent-based model on a network remains unknown.

In this study, we analytically investigate the effect of social reinforcement on transient fads in networked systems. To this end, we propose a simple multistage independent cascade (MIC) model, a multistage version of the IC model. The present MIC model is a discrete time fad model of $M = 2$. Provided that the underlying network is locally treelike, the tree approximation is applicable to this model. Here, we formulate the tree approximation for uncorrelated networks of arbitrary degree distribution p_k . As an application, we study this model on a random regular network of degree $k = 6$, random graphs, and scale-free networks, to show that the present model actually exhibits a discontinuous jump of the number of abandoners. We also investigate the percolation transitions in networks of susceptible nodes and abandoners. Interestingly, when the fraction of initial adopters is finite, the number of abandoners can discontinuously jump after the abandoner's network has percolated. Overall, the phase diagram of the MIC model crucially depends on the fraction of initial fad adopters.

2. Model

Consider a network of N nodes. In our MIC model, each node takes one of the four states: (0) susceptible and unaware, (1) informed (susceptible and aware), (2) fad adopter, and (3) fad abandoner. The model dynamics is given as follows (figure 1):

- (i) Randomly select a fraction ρ of nodes as the initial fad adopters (*seeds*). Set the state of other nodes to susceptible.
- (ii) Compile a (randomly ordered) list L of adopters. For each adopter (2) in L , compile a list S of the neighboring susceptible nodes (0 or 1). For each node in S , execute the following process: (ii-a) If the node is susceptible and unaware (0), change it to either informed ($0 \rightarrow 1$) with probability T_1 , fad adopter ($0 \rightarrow 2$) with probability T_2 , or leave unchanged otherwise. (ii-b) If the node is informed (1), change it to fad adopter ($1 \rightarrow 2$) with probability $T \equiv T_1 + T_2 (\leq 1)$, or leave unchanged. At this stage, the new adopters are not yet included in L .

- (iii) Change all adopters in L to abandoners ($2 \rightarrow 3$).
- (iv) Repeat (ii) and (iii) until no adopter exists in the network.

Note that when $T_1 = 0$, the model reduces to the IC model (the SIR model with transmissibility T_2).

In the following sections, we denote the final state fraction of nodes in states 0, 1, 2, and 3 by S_0 , S_1 , $S_2(= 0)$, and S_3 , respectively. We also designate the networks of susceptible nodes and abandoners as the S_0 -network and S_3 -network, respectively. The fractions of the largest components of the S_0 - and S_3 -networks are, respectively, denoted by S_0^{\max} and S_3^{\max} .

3. Phase Diagram in the $\rho \rightarrow 0$ limit

In this section, we consider the dynamics starting from an infinitesimal fraction of seeds ($\rho = 0+$) on uncorrelated networks with a given degree distribution p_k (for example, a random regular network, Erdős–Rényi random graph [30], or a scale-free network (SFN) generated by using the configuration model [31]). Newman analyzed the SIR model with transmissibility T (the present model with $T_1 = 0$ and $T_2 = T$) using generating functions [17, 32]. He reported two phase transitions as T is increased: a giant component of abandoners appears at the percolation threshold of the S_3 -network $T_c = \langle k \rangle / \langle k^2 - k \rangle$ (where $\langle \cdot \rangle$ denotes the average of a quantity weighted by p_k), and a giant component of susceptible nodes disappears at the percolation threshold of the S_0 -network $T_{c'}$. Correspondingly, there exist three distinct phases: $S_0^{\max} > 0$ and $S_3^{\max} = 0$ for $T < T_c$, $S_0^{\max} > 0$ and $S_3^{\max} > 0$ for $T_c < T < T_{c'}$, and $S_0^{\max} = 0$ and $S_3^{\max} > 0$ for $T > T_{c'}$. In the following, we generalize his method in order to apply it to the present model.

3.1. Percolation of the S_3 -network

We investigate the phase diagram of percolation (of the S_0 - and S_3 -networks), and therefore focus on the final state of the dynamics, where no adopters exist. Consider a randomly chosen (RC) node and its RC neighbor. Here we assume that the focal RC node was still susceptible or informed when the RC neighbor became an adopter (if such a neighbor exists). We denote the probability that the prompt of this RC neighbor did not change the state of the focal node by u , and the probability that the RC neighbor is susceptible or informed by v in the final state. Then u and v are related as

$$u = v + (1 - T)(1 - v) = 1 - T + Tv. \tag{1}$$

The first term v on the right-hand side of the first equality signifies that the RC neighbor did not adopt the fad and that no transmission occurred from this RC neighbor to the focal node. The second term $(1 - T)(1 - v)$ is the probability that the RC neighbor abandons the fad, but has never altered the state of the focal node while adopting the fad.

We can evaluate the fractions of each state, S_0 , S_1 , and S_3 , by u and v . To this end, it is convenient to introduce the generating function of the degree distribution p_k and the excess degree distribution q_k :

$$F_0(x) = \sum_k p_k x^k, \quad F_1(x) = \sum_k q_k x^k. \quad (2)$$

Here, q_k is the probability that an endpoint of an edge (an RC neighbor of an RC node) has excess degree k , i.e., the number of neighbors minus one is k . In uncorrelated networks, $q_k = (k+1)p_{k+1}/\langle k \rangle$, so that $F_1(x) = F_0'(x)/F_0'(1)$. Because the probability that an RC node with degree k is susceptible is u^k , the fraction of susceptible nodes S_0 , which is equal to the probability that an RC node is susceptible, is

$$S_0 = F_0(u) = \sum_k p_k u^k. \quad (3)$$

A node with degree k remained informed if it received information from just one of the adopters among its k neighbors and it did not receive any information from other neighbors. The probability that an RC neighbor was an adopter is $1-v$ and an informing attempt succeeds with probability T_1 . Therefore the probability that an RC node is informed is $\sum_k p_k \binom{k}{1} u^{k-1} (1-v) T_1 = T_1 (1-v) F_0'(u)$. Thus we obtain

$$S_1 = T_1 (1-v) F_0'(u). \quad (4)$$

Since $S_2 = 0$ in the final state, we have

$$S_3 = 1 - S_0 - S_1. \quad (5)$$

To obtain a self-consistent equation for u , we divide v into two parts, $v = v_0 + v_1$, where v_0 and v_1 are the probabilities that an RC neighbor of an RC node is susceptible and informed, respectively. Because u^k is the probability that an RC neighbor with excess degree k is susceptible and q_k is the excess degree distribution, we have

$$v_0 = F_1(u) = \sum_k q_k u^k. \quad (6)$$

Because the probability that an RC neighbor with excess degree k is informed is $\binom{k}{1} u^{k-1} (1-v) T_1$, we have

$$v_1 = T_1 (1-v) F_1'(u). \quad (7)$$

Adding v_0 and v_1 , we obtain

$$v = F_1(u) + T_1 (1-v) F_1'(u). \quad (8)$$

Equations (1) and (8) provide a self-consistent equation for u ,

$$u = 1 - T + T F_1(u) + T_1 (1-u) F_1'(u). \quad (9)$$

We now analyze in detail the solution of the self-consistent equation. For any value of T_1 and T_2 , there exists a trivial solution $u = 1$, implying that $S_0 = 1$, $S_1 = 0$, and thus $S_3 = 0$. To find nontrivial solutions, we solve equation (9) with respect to T_2 :

$$T_2 = \varphi_0(u; T_1) \equiv (1-u) \frac{1 + T_1 F_1'(u)}{1 - F_1(u)} - T_1. \quad (10)$$

This gives T_2 such that a given value of $u < 1$ is a solution of equation (9) with a fixed T_1 . For small $\bar{u} = 1 - u \ll 1$, equation (10) can be expanded to give

$$T_2 = \frac{1}{c_1} + \frac{c_2(1 - c_1 T_1)}{2c_1^2} \bar{u} + \frac{(3c_2^2 - 2c_1 c_3) + c_1(4c_1 c_3 - 3c_2^2)T_1}{12c_1^3} \bar{u}^2 + \dots, \quad (11)$$

where $c_n = F_1^{(n)}(1)$. Taking the limit $u \rightarrow 1 - (\bar{u} \rightarrow 0+)$, we have

$$T_2 = T_{2c} \equiv c_1^{-1} = \frac{1}{F_1'(1)} = \frac{\langle k \rangle}{\langle k^2 - k \rangle}, \quad (12)$$

above which the trivial solution $u = 1$ becomes unstable and S_3 is nonzero, implying that S_3^{\max} changes from $S_3^{\max} = 0$ to $S_3^{\max} > 0$.

The type of transition at $T_2 = T_{2c}$ depends on the value of T_1 . For fixed $T_1 < T_{2c}$, a nontrivial solution exists only for $T_2 > T_{2c}$ and $S_3 \rightarrow 0$ when $T_2 \rightarrow T_{2c}+$. Therefore $T_2 = T_{2c}$ is the continuous transition point of S_3 . For $T_1 > T_{2c}$, on the other hand, $u < 1$ is possible even when $T_2 < T_{2c}$. To see this, we consider small $\Delta_1 = T_1 - T_{2c}$ and $\Delta_2 = T_{2c} - T_2$ and let us rewrite equation (11) for

$$\Delta_2 = 2a\Delta_1 \bar{u} - b\bar{u}^2 + \dots, \quad (13)$$

where a and b are positive constants. When $\Delta_1 > 0$, Δ_2 can be positive for small $\bar{u} > 0$, yielding two branches of the nontrivial solution for $T_d^L < T_2 < T_d^U$ with

$$T_d^L \simeq T_{2c} - \frac{a^2}{b} \Delta_1^2, \quad T_d^U = T_{2c} \quad (14)$$

and the lower branch vanishes at T_d^U while the upper branch, which gives a positive S_3 , survives above T_d^U . By contrast, when $T_2 < T_d^L$, the trivial solution alone exists and the only possibility is $S_3 = 0$. This implies that S_3 *discontinuously* jumps from zero to the upper branch within the range $T_d^L \leq T_2 \leq T_d^U$. In general, T_d^L depends on T_1 and is given by $T_d^L(T_1) = \min_{0 < u < 1} \varphi_0(u; T_1)$.

3.2. Percolation of S_0 -network

When T_2 increases with T_1 fixed, the S_0 -network gradually shrinks and finally disintegrates into numerous finite components at $T_2 = T_{2c}$. Here, we examine this percolation problem.

Consider an RC node and its RC neighbor. The probabilities that the RC neighbor is susceptible, informed, and an abandoner that failed to affect the focal node while an adopter are v_0 , v_1 , and $(1-T)(1-v)$, respectively. The probability that a node in the S_0 -network has m susceptible neighbors, i.e., the degree distribution π_m of the S_0 -network, is represented as $\pi_m \propto \sum_{k=m}^{\infty} p_k \binom{k}{m} v_0^m [v_1 + (1-T)(1-v)]^{k-m}$. The corresponding generating function is

$$G_0(x) = \sum_m \pi_m x^m = \frac{F_0[v_0 x + v_1 + (1-T)(1-v)]}{F_0(u)} = \frac{F_0[v_0(x-1) + u]}{F_0(u)}. \quad (15)$$

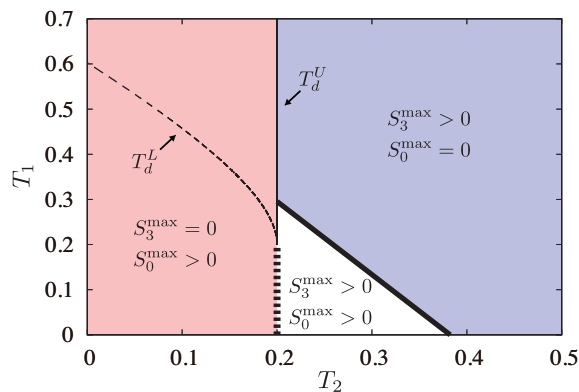


Figure 2. Phase diagram for the case $\rho = 0+$. The thick-solid and thick-dashed lines denote the continuous transition lines for the percolation of the S_0 -network $T_{2c'}$ and the S_3 -network T_{2c} , respectively. The thin-solid and thin-dashed lines denote the upper (T_d^U) and lower (T_d^L) bounds, respectively. Between these bounds, equation (9) has two nontrivial solutions.

Here the denominator is the prior probability of being susceptible. Similarly, the generating function for the excess degree distribution of the S_0 -network is derived as

$$G_1(x) = \frac{G'_0(x)}{G'_0(1)} = \frac{F_1[v_0(x-1) + u]}{F_1(u)}. \quad (16)$$

Because the mean excess degree of the S_0 -network is given by $G'_1(1)$, u at the percolation threshold $T_{2c'}$ (for a given T_1) satisfies

$$1 = G'_1(1) = v_0 \frac{F'_1(u)}{F_1(u)} = F'_1(u). \quad (17)$$

By following [32], we have the largest component of the S_0 -network. The fraction of the largest component in the S_0 -network, C , is

$$C = 1 - G_0(v_S), \quad (18)$$

where v_S is the probability that an S_0 -component connected by an RC edge is finite,

$$v_S = G_1(v_S). \quad (19)$$

Then the fraction of the largest component of the S_0 -network over the *whole network*, i.e., S_0^{\max} , is given as

$$S_0^{\max} = CS_0 = S_0(1 - G_0(v_S)). \quad (20)$$

3.3. Phase diagram for random regular network

We now consider the phase diagram of the present model on a degree-6 random regular network. Figure 2 shows the phase diagram in T_1 - T_2 space obtained by applying the tree approximation. The transition line of the S_3 -percolation is independent of T_1 and locates at $T_2 = T_{2c} = 1/(k-1) = 0.2$. However, the order of the transition is continuous when $T_1 < T_{2c}$, and otherwise discontinuous. In figure 3 (a), we plot S_3 as a function of

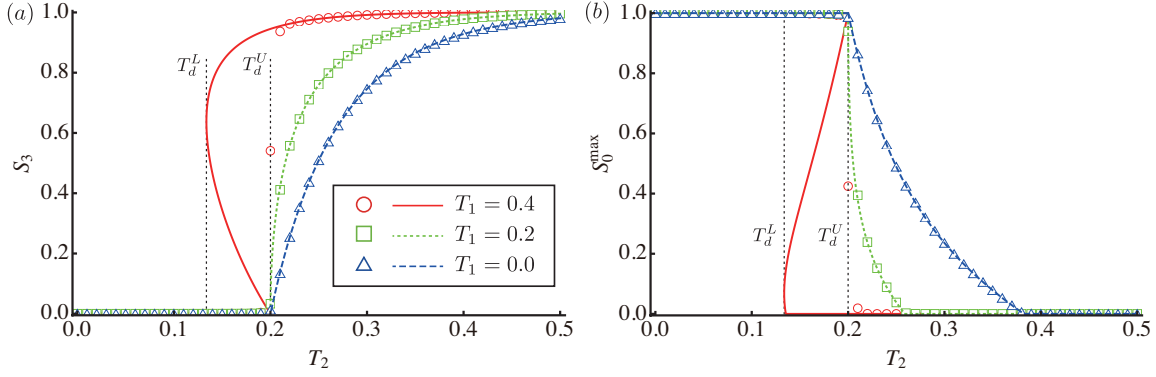


Figure 3. Analytical results (lines) for (a) S_3 and (b) S_0^{\max} as a function of T_2 with $T_1 = 0, 0.2,$ and 0.4 . T_d^L and T_d^U indicate the lower and upper bounds, respectively. Between these bounds, equation (9) has two nontrivial solutions. Symbols are obtained by Monte-Carlo simulations with very small $\rho (= 0.0001)$. The number of nodes used is $N = 256000$, and 100 trials for each of 100 graph realizations are used for averaging.

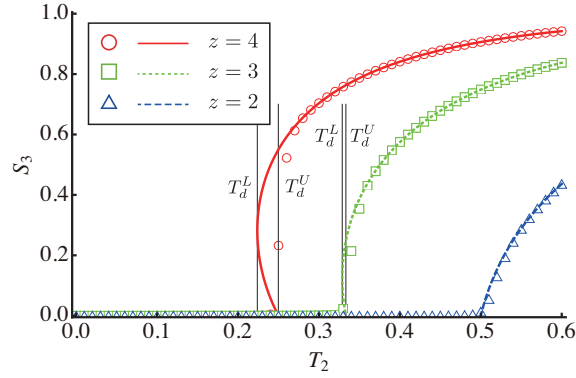


Figure 4. Analytical result (lines) for S_3 of the random graph, as a function of T_2 , for $T_1 = 0.4$ and several values of average degree z . Symbols are obtained by Monte-Carlo simulations with very small $\rho (= 0.0001)$. The number of nodes used is $N = 256000$, and 100 trials for each of 100 graph realizations are used for averaging.

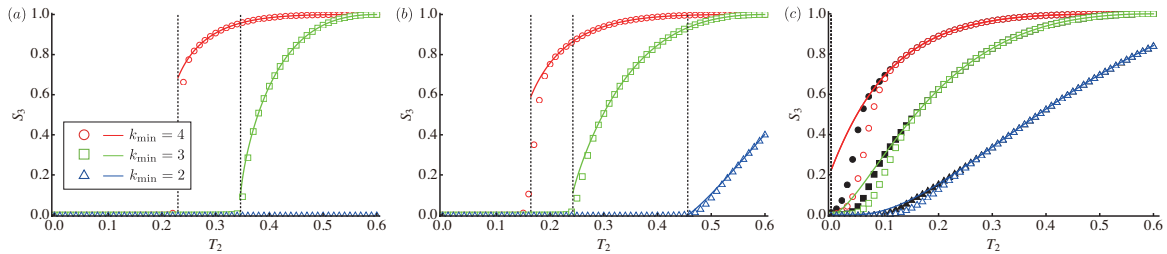


Figure 5. Analytical result (lines) for S_3 of the uncorrelated SFN with $T_1 = 0.4$ and several values of k_{\min} , as a function of T_2 . In each panel, the degree exponent γ is set to (a) $\gamma = 5$, (b) $\gamma = 4$, and (c) $\gamma = 3$, respectively. The vertical lines represent T_{2c} . Open symbols are the numerical results of S_3 obtained by Monte-Carlo simulations with very small $\rho (= 0.0001)$. The number of nodes used is $N = 256000$, and 100 trials for each of 100 graph realizations are used for averaging. The full symbols in (c) denote S_3 obtained by the Monte-Carlo simulations with a larger system size ($N = 1024000$).

T_2 for several values of T_1 . When T_1 is large, S_3 is multivalued in $T_d^L < T_2 < T_d^U = T_{2c}$. Since the dynamics begins from an infinitesimal fraction of seeds, S_3 remains at the lower branch for $T_2 < T_d^U$ and jumps to the upper branch at T_d^U , implying that a discontinuous occurrence of the giant component of the S_3 -network. Such a jump disappears when $T_1 < T_{2c}$. In figure 3(a), we also plot the numerical results obtained by the Monte-Carlo simulations. Our Monte-Carlo results with very small $\rho (= 0.0001)$ correspond well with the analytical calculations. The N - and ρ -dependence of the Monte-Carlo results will be checked later in figures 7 and 10, respectively.

For small T_1 (the blue-triangles and green-squares in figure 3(b)), giant components of the S_0 - and S_3 -networks coexist in $T_{2c} < T_2 < T_{2c'}$. This region shrinks with increasing T_1 , and $T_{2c'}(T_1)$ reaches T_{2c} at a certain value of T_1 ($T_1 \simeq 0.295$). Above this value (the red-circles in figure 3(b)), the S_3 -network percolates and the giant component of the S_0 -network simultaneously vanishes at $T_2 = T_{2c}$. The tricritical point (T_{2c}, T_{2c}) of the random regular network with degree k is given by $(1/(k-1), 1/(k-1))$. We note that $(T_{2c}, T_{2c}) = (0.5, 0.5)$ when $k = 3$, precluding $T_1 > T_{2c}$ at $T_2 = T_{2c}$ since $T = T_1 + T_2 \leq 1$. Consequently, the present model on a degree-3 random regular network exhibits only a continuous transition of the S_3 -network; discontinuous transitions are disallowed.

We now remark on other typical locally treelike networks; namely, the random graph with $p_k = e^{-z} z^k / k!$ and the uncorrelated SFN with $p_k = k^{-\gamma} / \sum_{k=k_{\min}} k^{-\gamma}$, where k_{\min} is the minimum degree.

For random graphs with average degree z , the generating functions are given as $F_0(x) = F_1(x) = \exp[z(x-1)]$, and the tricritical point (T_{2c}, T_{2c}) is given by $(1/z, 1/z)$. Thus, the MIC model undergoes a discontinuous transition when $z > 2$ rather than when $z > 3$. Figure 4 shows the analytical and numerical results for S_3 as a function of T_2 with $T_1 = 0.4$ and $z = 4, 3$, and 2. Numerical results support the validity of our tree approximation, while it is hard to assess numerically the discontinuity of S_3 when $z = 3$ because the interval of $T_d^L < T_2 < T_d^U$ is very narrow.

Figure 5 shows the analytical and numerical results for S_3 of the uncorrelated SFN with $T_1 = 0.4$ and several values of γ and k_{\min} . For the case of $\gamma = 5$, S_3 discontinuously jumps at T_{2c} when $k_{\min} = 3, 4$ (although the discontinuity at $k_{\min} = 3$ is weak as well as the random graph with $z = 3$), but S_3 is always zero when $k_{\min} = 2$, where $T_{2c} = 1/F_1'(1) > 0.6$. For the case of $\gamma = 4$, S_3 can be nonzero even when $k_{\min} = 2$. But the transition at T_{2c} is continuous one because $T_{2c} \simeq 0.456 > T_1 (= 0.4)$. We have a discontinuous jump of S_3 when $k_{\min} = 3, 4$. For the case of $\gamma = 3$, $T_{2c} = 0$ because $F_1'(1) = \langle k^2 - k \rangle / \langle k \rangle$ diverges irrespectively of k_{\min} . Therefore, both continuous and discontinuous transition lines of the S_3 -network disappear, and only the percolation transition of the S_0 -network exists. Monte-Carlo simulations for the case of $\gamma = 3$ suffer a finite size effect in a small T_2 -region, although the deviation from the analytical lines will vanish with increasing N (see the full symbols in figure 5(c)).

4. Sensitivity to the fraction of initial adopters

4.1. Tree approximation

From the formal analysis in the previous section, we can easily derive the self-consistent equations when the fraction of initial adopters $\rho > 0$. Let $\bar{\rho} = 1 - \rho$ be the initial fraction of susceptible nodes. In the present model, $v = v_0 + v_1$ where

$$v_0 = \bar{\rho}F_1(u), \quad v_1 = \bar{\rho}T_1(1 - v)F'_1(u), \quad (21)$$

and the relationship $u = 1 - T + Tv$ is unchanged. Thus, we obtain an expression in u alone:

$$u = 1 - T(1 - \bar{\rho}F_1(u)) + \bar{\rho}T_1(1 - u)F'_1(u). \quad (22)$$

By using the solution, we obtain

$$S_0 = \bar{\rho}F_0(u), \quad S_1 = \bar{\rho}T_1(1 - v)F'_0(u) = \bar{\rho}\frac{T_1(1 - u)}{T}F'_0(u), \quad (23)$$

and $S_3 = 1 - S_0 - S_1$.

When $\rho > 0$, there is no trivial solution of equation (22) for all regions of parameters and no continuous transition in the sense that S_3 is always nonzero because $S_3 \geq \rho > 0$. Nevertheless, the percolation of the S_3 -network (from $S_3^{\max} = 0$ to $S_3^{\max} > 0$) can take place as long as ρ is smaller than the percolation critical density (as shown in the next subsection). Moreover, a discontinuous jump of S_3 is still possible. Equation (10) is modified to

$$T_2 = \varphi_\rho(u; T_1) = (1 - u)\frac{1 + \bar{\rho}T_1F'_1(u)}{1 - \bar{\rho}F_1(u)} - T_1, \quad (24)$$

and the lower and upper bounds of the discontinuous point (T_d^L and T_d^U , respectively) can be given by the local minimum and local maximum of $\varphi_\rho(u; T_1)$ in $0 < u < 1$, respectively. Depending on T_1 , there exists some ρ , above which $\varphi_\rho(u; T_1)$ is monotonically decreasing and these bounds do not exist (figure 11).

On the S_0 -network, the percolation threshold $T_{2c}(T_1)$ and the ratio of the largest component S_0^{\max} are derived in the same manner; that is, (17) and (20) remain valid, along with (21) and (23).

4.2. Results for random regular network

We now discuss the sensitivity of the phase diagram to the fraction of initial adopters on a degree-6 random regular network. Here, we verified our analytical results by Monte-Carlo simulations of the present model. The number of nodes used is $N = 4000, 16000, 64000,$ and 256000 . The number of graph realizations, and also the number of trials on each graph are 100.

Figure 6 plots the phase diagram when $\rho = 0.01$. The lower and upper bounds ($T_d^L(T_1)$ and $T_d^U(T_1)$) of the discontinuous jump of the S_3 -network and the percolation threshold ($T_{2c}(T_1)$) of the S_0 -network are drawn by the tree approximation. Moreover,

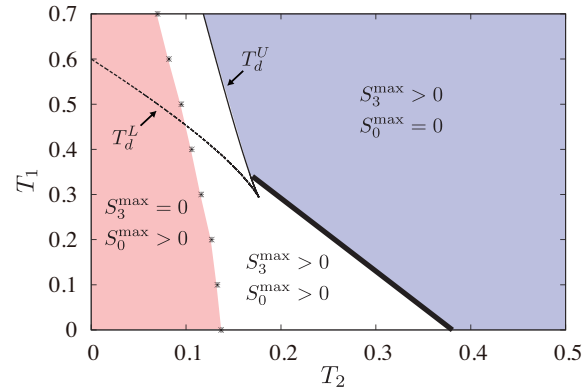


Figure 6. Phase diagram for the case $\rho = 0.01$. The thin-solid and thin-dashed lines denote the upper (T_d^U) and lower (T_d^L) bounds, respectively. Between these bounds, equation (22) has two nontrivial solutions. The thick-dashed line denotes the transition line of percolation of the S_0 -network T_{2c} . Discrete dots denote the percolation transition points of the S_3 -network obtained by Monte-Carlo simulations.

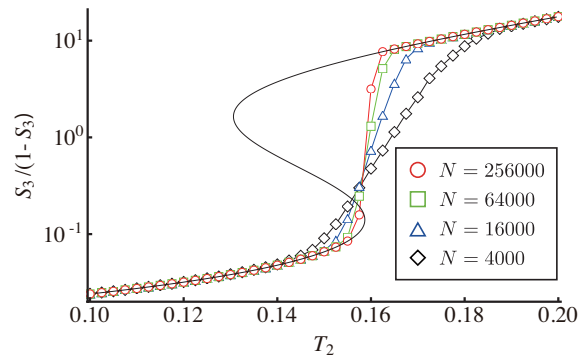


Figure 7. S_3 as a function of T_2 for $T_1 = 0.4$ and $\rho = 0.01$. The analytic result (solid curve) and the result obtained by simulation are shown. Here, S_3 is rescaled to $S_3/(1 - S_3)$ for observing the behaviors near $S_3 = 0$ and 1. The analytical evaluation gives $T_d^L \simeq 0.131$ and $T_d^U \simeq 0.159$.

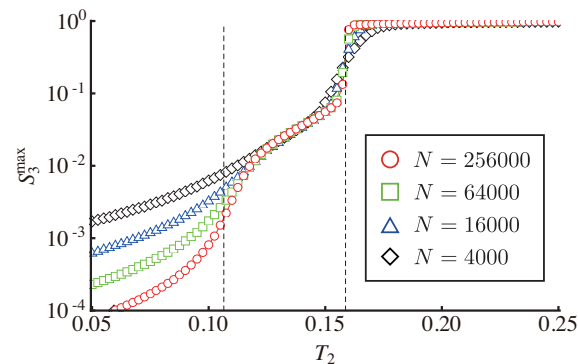


Figure 8. Monte-Carlo results of S_3^{\max} as a function of T_2 , with $T_1 = 0.4$ and $\rho = 0.01$. The two vertical lines represent $T_{2c} \simeq 0.106$ and $T_d^U \simeq 0.159$. $T_{2c} \simeq 0.106$ is given by the cross point of the effective fractal exponents of differently sized systems.

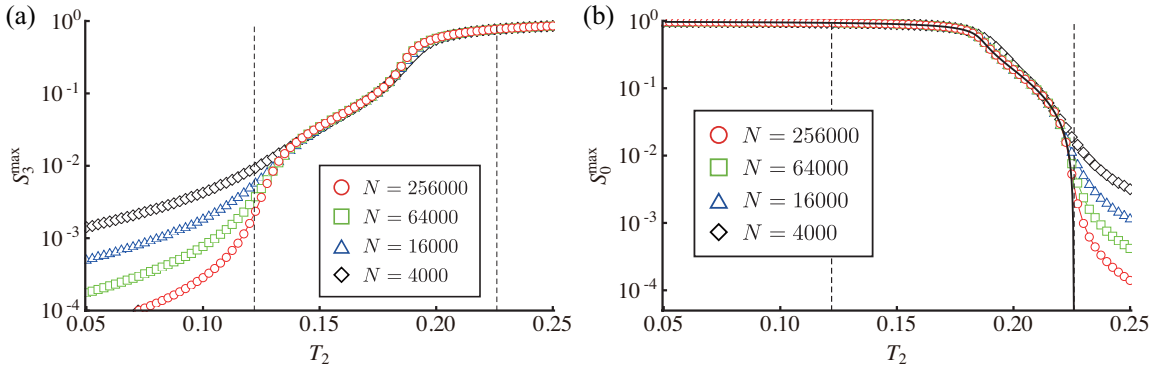


Figure 9. Monte–Carlo results for (a) S_3^{\max} and (b) S_0^{\max} as functions of T_2 , with $T_1 = 0.25$ and $\rho = 0.01$. The two vertical lines represents $T_{2c} \simeq 0.122$ and $T_{2c'} \simeq 0.226$. Here, T_{2c} is given by the cross point of the fractal exponents of differently sized systems. The solid line in (b) is drawn by equation (20), which gives $T_{2c'}$. Note the lack of any discontinuous jump of S_3 (figure 6).

plotted (discrete dots) are the numerically estimated percolation transition points $T_{2c}(T_1)$ of the S_3 -network, where S_3^{\max} changes from $S_3^{\max} = 0$ to $S_3^{\max} > 0$. Each transition point is estimated from the cross point of the effective fractal exponent $\psi(N)$ [33], defined as $\psi(N) = d \ln N S_3^{\max}(N) / d \ln N$. Note that the existence of the crossing point of the effective fractal exponents for various N indicates a continuous transition [33, 34].

This phase diagram is crucially different from that of $\rho = 0+$. For $\rho > 0$, the upper bound $T_d^U(T_1)$ deviates from the vertical line $T_2 = 0.2$ (i.e., the discontinuous transition line of the case $\rho = 0+$). The continuous transition points $T_{2c}(T_1)$ of the S_3 -network at small T_1 move toward the lower side and never intercept the upper bound $T_d^U(T_1)$ at large T_1 . Then the percolation of the S_3 -network and the discontinuous jump of S_3 occur at different points: as T_2 increases with a fixed value of T_1 (> 0.294 for $\rho = 0.01$), a continuous transition of the S_3 -network occurs, followed by a discontinuous change in S_3 as T_2 approaches the upper bound $T_d^U(T_1)$.

Figure 7 compares the analytical and numerical results for S_3 with $T_1 = 0.4$. Both results nearly coincide except near the discontinuous transition point $T_2 = T_d^U \simeq 0.159$. As T_2 increases, S_3 rapidly changes from the lower to the upper branch, the cross-over becomes sharpens and steepens, and the location becomes closer to T_d^U as N increases, indicating that the rapid change occurs as a sudden jump at T_d^U in the large size limit. The size dependence of apparent crossing points also shows that the crossing point approaches T_d^U as N increases (not shown). The fraction of the largest component S_3^{\max} also changes discontinuously at T_d^U (figure 8).

Discontinuous transitions never appear at small T_1 , in either the analytical or numerical solutions (the case of $T_1 = 0.25$ is plotted in figure 9). In this case, the S_3 -network first percolates ($T_{2c} \simeq 0.122$ for $T_1 = 0.25$), then continuously increases to $S_3 = 1$ (figure 9(a)). Figure 9(b) plots the Monte–Carlo result of S_0^{\max} with $T_1 = 0.25$

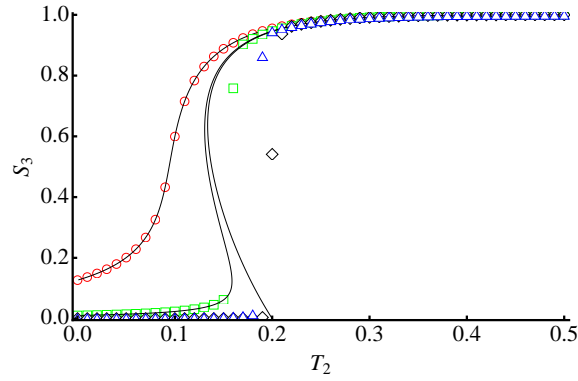


Figure 10. Analytically determined S_3 as a function of T_2 with $T_1 = 0.4$ and $\rho = 0, 0.01, \text{ and } 0.1$ (right to left). Symbols are Monte-Carlo results of $N = 256000$ and $\rho = 0.1$ (red-circles), 0.01 (green-squares), 0.001 (blue-triangles), and 0.0001 (black-diamonds).

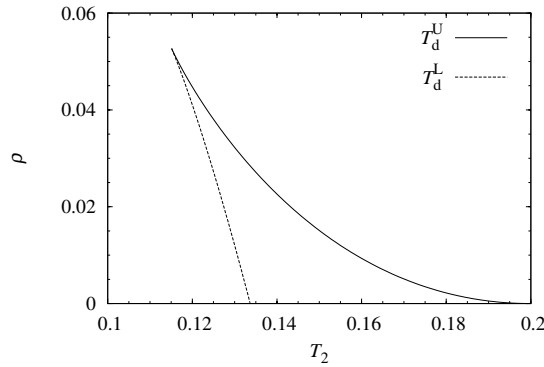


Figure 11. Analytically determined lower and upper bounds of discontinuous jumps in the T_2 - ρ plane with $T_1 = 0.4$.

and $\rho = 0.01$. The numerically evaluated S_0^{\max} are well fitted by equation (20), implying that the S_0 -network disintegrates at $T_{2c'}(T_1) (> T_d^U(T_1))$ when $T_1 < 0.344$, as analytically determined. When $T_1 > 0.344$, the percolation transition of the S_0 -network occurs simultaneously with a discontinuous jump of S_3 .

Finally, analytical curves of S_3 versus T_2 , for fixed $T_1 = 0.4$ and various values of ρ , are plotted in figure 10. When ρ is small, a precursor of the discontinuous S_3 jump is seen, similar to in figure 3. This behavior disappears as ρ increases. Figure 11 plots the analytically determined lower and upper bounds over a range of ρ . As noted in the previous subsection, a critical fraction $\rho_c \simeq 0.053$ exists at $T_1 = 0.4$, above which both bounds of discontinuous jump disappear and the system exhibits only continuous transitions of percolations of the S_3 -and S_0 -networks.

5. Summary

We have investigated an MIC model on networks. Using the tree approximation, we derived formulas for evaluating S_0 , S_1 , and S_3 and thus constructed the phase diagram. As an application, we studied the phase diagram of the present model on several networks, and confirmed agreement between the results and our analytical predictions. In particular, the abandoners discontinuously percolated at large T_1 . Moreover, when the dynamics began from a finite fraction of initial adopters, the discontinuous jump in the number of abandoners occurred after the percolation of the abandoner. It is not until the present MIC model is placed *on a network* that we can observe the last behavior. As to the original fad model proposed by Krapivsky et al., we find a similar behavior, “*a discontinuous jump after the percolation*” when the fad model is placed on a network [36].

Our tree approximation for the present MIC model is valid only on uncorrelated networks. Investigating the relationship between the cooperative behavior of the model and the properties of the network on which the dynamics is performed (e.g., clustering, degree correlation, and community structure) is beyond the scope of this study. For example, clustering decreases the threshold of the SIR model [35], but an innovation in the linear threshold model is more easily propagated in clustered networks than in random networks [12, 8]. How the MIC model behaves in clustered networks requires further research.

Acknowledgments

This work was partially supported by the Grant-in-Aid for Young Scientists (B) of Japan Society for the Promotion of Science (Grant No. 24740054 to T.H.) and JST, ERATO, Kawarabayashi Large Graph Project.

Reference

- [1] Granovetter M 1978 *Am. J. Sociol.* **83** 1420.
- [2] Schelling T C 1978 *J. Conflict. Resolut.* **17** 381.
- [3] Valente T W 1995 *Network Models of the Diffusion of Innovations* (Hampton Press, Cresskill, NJ).
- [4] Mahajan V, Muller E, and Bass F M 1990 *J. Marketing* **54** 1.
- [5] Bikhchandani S, Hirshleifer D, and Welch I 1992 *J. Polit. Econ.* **100** 992.
- [6] Watts D J 2002 *Proc. Natl. Acad. Sci. USA* **99**, 5766.
- [7] Watts D J and Dodds P S 2007 *J. Consum. Res.* **34** 441.
- [8] Centola D, Eguíluz V M, and Macy M W 2007 *Physica A* **374** 449.
- [9] Gleeson J P and Cahalane D J 2007 *Phys. Rev. E* **75** 056103.
- [10] Gleeson J P 2008 *Phys. Rev. E* **77** 046117.
- [11] Payne J L, Dodds P S, and Eppstein M J 2009 *Phys. Rev. E* **80** 026125.
- [12] Ikeda Y, Hasegawa T, and Nemoto K 2010 *J. Phys. Conf. Ser.* **221** 012005.
- [13] Hackett A, Melnik S, and Gleeson J P 2011 *Phys. Rev. E* **83** 056107.
- [14] Anderson R M and May R M 1992 *Infectious Diseases of Humans: Dynamics and Control* (Oxford University press).

- [15] Goldenberg J, Libai B, and Muller E 2001 *Acad. Market. Sci. Rev.*, **9**, 1–18
- [16] Kempe D, Kleinberg J, and Tardos É 2003 *Proc. 9th ACM SIGKDD Int. Conf. on Knowledge Discovery and Data Mining* 137–146.
- [17] Newman M E J 2002 *Phys. Rev. E* **66** 016128.
- [18] Pastor-Satorras R and Vespignani A 2001 *Phys. Rev. Lett.* **86** 3200.
- [19] Pastor-Satorras R and Vespignani A 2001 *Phys. Rev. E* **63** 066117.
- [20] Tomé T and Ziff R M 2010 *Phys. Rev. E* **82** 051921.
- [21] Kenah E and Robins J M 2007 *Phys. Rev. E* **76** 036113.
- [22] Miller J C 2007 *Phys. Rev. E* **76** 010101.
- [23] Kenah E and Miller J C 2011 *Interdiscip. Perspect. Infect. Dis.* 543520.
- [24] Dodds P S and Watts D J 2004 *Phys. Rev. Lett.* **92** 218701.
- [25] Antal T and Krapivsky P L 2012 *J. Stat. Mech.* P07018.
- [26] de Kerchove C, Krings G, Lambiotte R, Van Dooren P, and Blondel V D 2009 *Phys. Rev. E* **79** 016114.
- [27] Melnik S, Ward J, Gleeson J, and Porter M 2013 *Chaos* **23** 013124.
- [28] Krapivsky P L, Redner S, and Volovik D 2011 *J. Stat. Mech.* P12003.
- [29] Starnini M, Baronchelli A, and Pastor-Satorras R 2012 *J. Stat. Mech.*, P10027.
- [30] Erdős P and Rényi A 1960 *Publ. Math. Inst. Hung. Acad. Sci.* **5** 17.
- [31] Molloy M and Reed B 1995 *Random Struct. Algorithms* **6** 161.
- [32] Newman M E J 2005 *Phys. Rev. Lett.* **95** 108701.
- [33] Hasegawa T, Nogawa T, and Nemoto K 2013 *EPL* **104** 16006.
- [34] Nogawa T and Hasegawa T 2014 *Phys. Rev. E* **89** 042803.
- [35] Newman M E J 2003 *Phys. Rev. E* **68** 026121.
- [36] Hasegawa T, Kinoshita N, and Nemoto K in preparation.